

# High-Purity Diamagnetic Single-Wall Carbon Nanotube Buckypaper

Younghyun Kim,<sup>†</sup> Omar N. Torrens,<sup>‡</sup> J. M. Kikkawa,<sup>‡</sup> Edy Abou-Hamad,<sup>§</sup>  
Christophe Goze-Bac,<sup>§</sup> and David E. Luzzi<sup>\*,†</sup>

Department of Materials Science and Engineering and Department of Physics and Astronomy, University of Pennsylvania, Philadelphia, Pennsylvania 19104-6272, LCVN, Institut de Physique de Montpellier, CNRS Université Montpellier 2, 34090 Montpellier, France

Received December 18, 2006. Revised Manuscript Received March 1, 2007

We describe a novel purification process for single-wall carbon nanotube (SWNT) materials that removes non-nanotube carbon and reduces ferromagnetic impurities to levels at which native SWNT magnetic properties predominate. Ferromagnetism is reduced from 1.04 to less than 0.013 emu/g by magnetic gradient filtration. This procedure creates samples of sufficient quality for spectroscopies such as nuclear magnetic resonance (NMR). The overall cleanliness and purity of the material is confirmed through NIR absorption spectroscopy, X-ray diffraction, C<sub>60</sub> filling experiments with yields exceeding 90%, and high-resolution <sup>13</sup>C NMR.

## Introduction

Single-wall carbon nanotubes (SWNTs) have generated significant interest because of their unique electrical, thermal, and mechanical properties.<sup>1–3</sup> These superior characteristics can be compromised in the presence of impurities, such as amorphous carbon or ferromagnetic catalyst particles, which are introduced during synthesis. For example, the electron spin resonance (ESR) signal is absent in catalyst-containing samples,<sup>4</sup> and a similar effect is seen for nuclear magnetic resonance (NMR) in which a broad line with about 1500 ppm of anisotropy is observed for nonpurified SWNT materials.<sup>5,6</sup> Measurement of the specific heat is obscured at low temperature because of nuclear hyperfine interactions in metallic impurities.<sup>7</sup> Small amounts of magnetic impurities can also influence nanotube electrical properties through Kondo-like interactions with conduction electrons.<sup>8,9</sup>

Various purification methods have been employed to remove magnetic impurities, such as chemical treatment,

microwave heating, mechanical filtration, and heat treatment in a vacuum or oxidative environment.<sup>10–13</sup> However, a graphitic coating commonly found around ferromagnetic catalyst particles shields the particles from acid dissolution. Attempts to remove this graphitic coating often result in damage or destruction of SWNTs.<sup>13</sup> Although some groups applied magnetic filtration, the efficiency was low such that ferromagnetism still dominated the magnetic moment of the sample for fields of order a few Tesla.<sup>14–17</sup> To circumvent this problem, other researchers synthesized nanotubes using non-ferromagnetic catalysts such as Rh/Pd or Rh/Pt.<sup>5,18</sup> Although this enables an NMR investigation of the nanotubes, the thermal and electrical properties are still dominated by the metallic catalyst particles. Also, the small diameter (average of 0.85 nm) of these nanotubes renders them unsuitable for endohedral filling, which is an interesting way to functionalize nanotubes. By using isotopically enriched <sup>13</sup>C, researchers have made SWNT materials from which NMR signals can be observed after magnetic processing using standard techniques common to biochemical fields.<sup>19</sup>

\* Corresponding author. Tel: 215-898-8366. Fax: 215-573-2128. E-mail: luzzi@lrsm.upenn.edu.

<sup>†</sup> Department of Materials Science and Engineering, University of Pennsylvania.

<sup>‡</sup> Department of Physics and Astronomy, University of Pennsylvania.

<sup>§</sup> CNRS Université Montpellier.

- (1) Vavro, J.; Kikkawa, J. M.; Fischer, J. E. *Phys. Rev. B* **2005**, *71*, 155410.
- (2) Hone, J.; Batlogg, B.; Benes, Z.; Johnson, A. T.; Fischer, J. E. *Science* **2000**, *289*, 1730.
- (3) Jaroenapibal, P.; Luzzi, D. E.; Evoy, S. *Appl. Phys. Lett.* **2004**, *85*, 4328.
- (4) Claye, A. S.; Nemes, N. M.; Janossy, A.; Fischer, J. E. *Phys. Rev. B* **2000**, *62*, R4845.
- (5) Tang, X. P.; Kleinhammes, A.; Shimoda, H.; Fleming, L.; Bennoune, K. Y.; Sinha, S.; Bower, C.; Zhou, O.; Wu, Y. *Science* **2000**, *288*, 492.
- (6) Goze-Bac, C.; Latil, S.; Vaccarini, L.; Bernier, P.; Gaveau, P.; Tahir, S.; Micholet, V.; Aznar, R.; Rubio, A.; Metenier, K.; Beguin, F. *Phys. Rev. B* **2001**, *63*, 100302.
- (7) Lasjaunias, J. C.; Biljakovic, K.; Benes, Z.; Fischer, J. E.; Monceau, P. *Phys. Rev. B* **2002**, *65*, 113409.
- (8) Grigorian, L.; Sumanasekera, G. U.; Loper, A. L.; Fang, S. L.; Allen, J. L.; Eklund, P. C. *Phys. Rev. B* **1999**, *60*, R11309.
- (9) Gracia, R. S.; Nieuwenhuizen, T. M.; Lerner, I. V. *Europhys. Lett.* **2004**, *66*, 419.

- (10) Rinzler, A. G.; Liu, J.; Dai, H.; Nikolaev, P.; Huffman, C. B.; Rodriguez-Macias, F. J.; Boul, P. J.; Lu, A. H.; Heymann, D.; Colbert, D. T.; Lee, R. S.; Fischer, J. E.; Rao, A. M.; Eklund, P. C.; Smalley, R. E. *Appl. Phys. A* **1998**, *67*, 29.
- (11) Strong, K. L.; Anderson, D. P.; Lafdi, K.; Kuhn, J. N. *Carbon* **2003**, *41*, 1477.
- (12) Harutyunyan, A. R.; Pradhan, B. K.; Chang, J.; Chen, G.; Eklund, P. C. *J. Phys. Chem. B* **2002**, *106*, 8671.
- (13) Zhou, W.; Ooi, Y. H.; Russo, R.; Papanek, P.; Luzzi, D. E.; Fischer, J. E.; Bronikowski, M. J.; Willis, P. A.; Smalley, R. E. *Chem. Phys. Lett.* **2001**, *350*, 6.
- (14) Thien-Nga, L.; Hernadi, K.; Ljubovic, E.; Garaj, S.; Forro, L. *Nano Lett.* **2002**, *2*, 1349.
- (15) Wiltshire, J. G.; Li, L. J.; Kholbystov, A. N.; Padbury, C. J.; Briggs, G. A. D.; Nicholas, R. J. *Carbon* **2005**, *43*, 1151.
- (16) Islam, M. F.; Milkie, D. E.; Torrens, O. N.; Yodh, A. G.; Kikkawa, J. M. *Phys. Rev. B* **2005**, *71*, 201401(R).
- (17) Kim, Y.; Luzzi, D. E. *J. Phys. Chem. B* **2005**, *109*, 16636.
- (18) Goze-Bac, C.; Latil, S.; Lauginie, P.; Jourdain, V.; Conard, J.; Duclaux, L.; Rubio, A.; Bernier, P. *Carbon* **2002**, *40*, 1825.
- (19) Kitaygorodskiy, A.; Wang, W.; Xie, S.-Y.; Lin, Y.; Shiral Fernando, K. A.; Wang, X.; Qu, L.; Chen, B.; Sun, Y.-P. *J. Am. Chem. Soc.* **2005**, *127*, 7517.

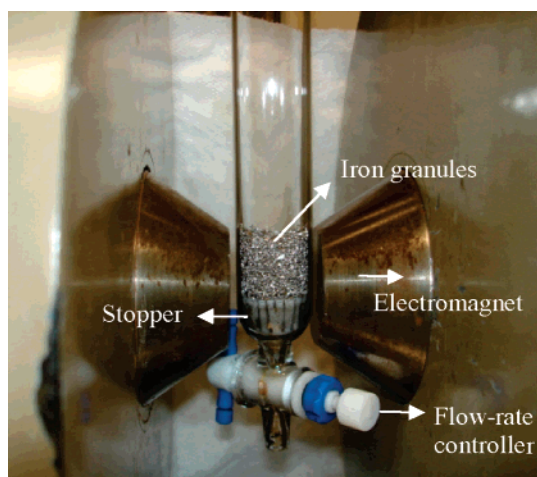


**Figure 1.** The magnetic gradient filtration setup.

These purification methods are insufficient to achieve the levels of purity necessary for electric and thermal applications and for the study of standard nonenriched nanotube materials. The high cost and low yield of SWNT materials provided by these methods make them ill-suited for mass production.

In this paper, we present a new purification regimen that successfully removes  $\sim 99\%$  of ferromagnetic or superparamagnetic impurities, yielding diamagnetic nanotube samples while also improving overall sample purity. Our method combines conventional air oxidation and chemical treatments with magnetic gradient filtration. In magnetic gradient filtration, a suspension containing the nanotubes is passed through a bed of iron beads in the presence of a 1.1 T magnetic field. A locally inhomogeneous magnetic field, which is produced around the iron beads, is used to trap remnant magnetic impurities. Ferromagnetic catalyst particles, which have survived chemical purification due to the presence of a protective graphitic coating, are attracted to the iron beads with a magnetic force  $F = \nabla(\vec{\mu} \cdot \vec{B})$ , where  $\vec{\mu}$  is the magnetic moment of the particle and  $\vec{B}$  is the magnetic field whose local gradient is maximized by the iron beads. The method also works efficiently with suspensions of larger diameter SWNTs that can subsequently be filled with molecules to form high-purity, bulk “peapod” materials.

### Experimental Section

We obtained SWNT samples from Carbon Solutions (PII-SWNTs) produced by the electric arc discharge technique using a Ni/Y catalyst in a 4:1 atomic percent ratio. As-received materials were already subjected to proprietary purification methods by the vendor and will heretofore be referred to as “pretreated.” Our purification procedure begins with oxidation in air at 560 °C for 10–30 min with a final yield of 40–60 wt %. The resulting materials are then sonicated in concentrated hydrochloric acid (37.3%) at 60 °C for 40 min to dissolve bare catalyst particles, filtered through a 1.2  $\mu\text{m}$  polycarbonate membrane, washed with distilled water, and dried at 100 °C for 5 min. Next, we create suspensions by adding 0.1–0.2 mg/mL *N,N*-dimethylformamide (DMF) and sonicating at 60 °C for 3–5 h.

The dispersed SWNT solutions are filtered through a 1.1 T magnetic gradient apparatus (Figure 1) containing a 4 cm high filter bed of iron granules (99.98% purity, 1–2 mm, Alfa Aesar). The solutions are passed through the apparatus 3 times at progressively

slower rates (20, 10, and 3 mL/min) while iron granules are refreshed after each cycle. Finally, suspensions are filtered through a 0.45  $\mu\text{m}$  nylon membrane to recover the SWNTs, which are then annealed at 650 °C for 30 min in a dynamic vacuum ( $\sim 2 \times 10^{-6}$  Torr) to remove residual DMF. We refer to the resulting samples as “purified”. The instrumentation is laboratory scale; the purification starts with  $\sim 200$  mg of pretreated material and produces a final yield of 10–20 wt %.

A variety of methods are used to measure the effect of our purification procedure on impurity content. Magnetometry probes the permanent moments associated with residual catalyst particles and is performed in a Quantum Design physical property measurement system (PPMS). Thermogravimetric analysis (TGA) measures the total metal content (TA Instruments SDT 2960, ramp speed 10 °C/min at 70 sccm air flow), and the atomic constituents of the metal particles are identified using an Oxford energy dispersive X-ray spectrometer (EDS) on a scanning electron microscope (JEOL 6400). Estimation of the SWNT content in each sample is obtained using absorbance spectroscopy (Varian Cary 5000 UV–vis–NIR spectrophotometer) utilizing the rapid purity assessment method.<sup>20</sup> X-ray diffraction (XRD, copper  $K_{\alpha}$  X-ray with wavelength  $\lambda = 1.54$  Å) is used to measure the relative increase of the SWNT bundle content due to purification by normalizing to the residual content of graphitic nanoparticles and multiwall nanotubes. We also measure by XRD the fraction of bundled SWNTs that fill upon exposure to a vapor of  $C_{60}$  molecules, which is sensitive to surface cleanliness. As a final measure of sample quality, NMR experiments are performed in order to demonstrate the low catalyst content and to further characterize the magnetically purified materials. High-resolution  $^{13}\text{C}$  NMR spectra are recorded on an ASX200 Bruker spectrometer using magic angle spinning (MAS NMR). Spin lattice  $T_1$  relaxation is measured at room temperature by saturation recovery experiments to distinguish the contributions of metallic and semiconducting nanotubes.<sup>18</sup>

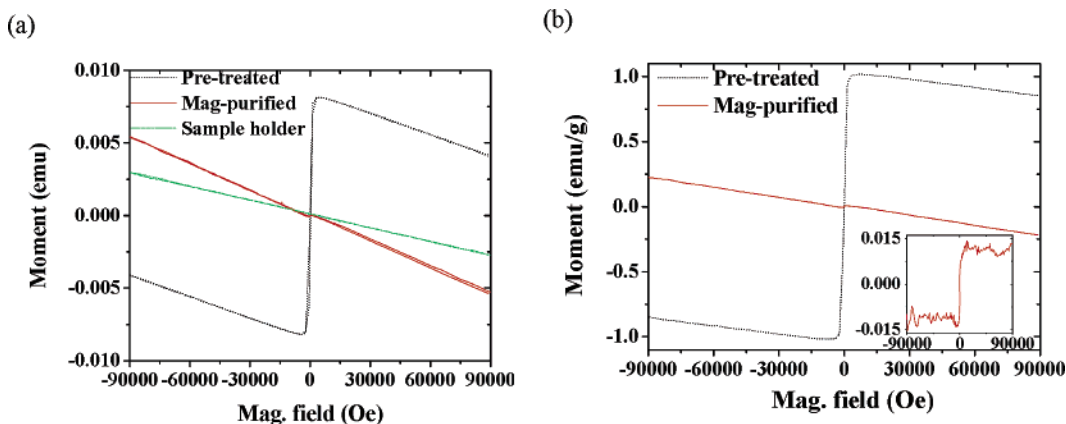
### Results

Figure 2 shows a dramatic reduction in ferromagnetic impurity content upon purification. To ensure the accuracy of these data, we purified a large quantity of SWNTs so the diamagnetic moment of the sample can be accurately resolved above the diamagnetic background of the sample holder. The relative diamagnetic contribution of the holder was approximately 50% that of the sample (Figure 2a) and varied less than 2.5% upon loading the holder 10 times.

Figure 2b shows the mass-normalized magnetic moment after subtraction of the sample holder contribution from the raw data. The pretreated sample is dominated by permanent moment contributions, whereas purified samples show a net diamagnetic response in fields exceeding 0.3 T. The saturation permanent moment is obtained by subtracting the high-field linear diamagnetic component from the mass-normalized magnetic moment as shown in the inset of Figure 2b. Purification reduces this moment nearly 2 orders of magnitude from 1.04 to 0.013 emu/g. We find reasonable agreement with the latter when material from six separately purified samples is combined to form a larger sample, yielding a permanent moment of 0.012 emu/g.

We also compare the overall purity of pretreated and magnetically purified materials using TGA, EDS, absorption

(20) Landi, B. J.; Ruf, H. J.; Evans, C. M.; Cress, C. D.; Raffaele, R. P. *J. Phys. Chem. B* **2005**, *109*, 9952.



**Figure 2.** (a) Raw magnetic hysteresis loops of pretreated SWNTs (8.18 mg, black line), magnetically purified SWNTs (11.56 mg, red line) and the empty sample holder (blue line). The Y-axis has units of raw emu, and is not divided by sample mass to explicitly reveal sample holder contributions to the raw data. (b) Mass-normalized magnetic moments of the pretreated sample (black line) and the magnetically purified sample (red line). The inset shows the saturated permanent moment of the remaining catalyst particles in the mag-purified material obtained by subtracting the linear diamagnetic response at high magnetic fields. Magnetization data are taken at  $T = 300$  K.

spectroscopy, and XRD. Metallic content is estimated from TGA assuming Ni and Y are oxidized to NiO and  $Y_2O_3$  during TGA up to 1000 °C and shows a reduction from 5–10 wt % in pretreated materials to 1.3% in purified samples. TGA residues are further weighed in an external microbalance to corroborate the TGA analysis. Because magnetic catalysts are metallic, it is surprising that metal content reduction during purification is within a single order of magnitude, whereas the permanent moment is reduced by nearly 2 orders of magnitude. To understand this discrepancy, we evaluated TGA residues by EDS. In each residue, two measurements are taken from separate areas, each measuring  $\sim 2500 \mu m^2$ , to ensure good statistics. Using internal standards, we find the Ni:Y ratio to be 20:1 in pretreated samples. This result is somewhat surprising because the material originates from an arc-furnace with a cored graphite rod containing a 4:1 Ni:Y ratio. It is not clear whether the synthesis process or the subsequent purification regimen used by Carbon Solutions Inc. for their PII-SWNT product are the source of this Ni enrichment. In any event, we find that our purification procedure reduces the Ni:Y ratio from 20:1 to 2:1. This disproportionate reduction in Ni content during magnetic purification could explain the larger proportional reduction in permanent moment versus metallic content, as discussed below.

Although developed for magnetic purification, our procedure also improves other benchmarks of sample purity and quality. Optical absorbance shows an improvement in SWNT abundance, XRD shows enhanced crystallinity indicating improved SWNT content, filling experiments show efficient formation of peapod structures indicating clean SWNT surfaces, and  $^{13}C$  MAS NMR confirms the absence of the ferromagnetic catalyst particles as well as the predominance of the clean SWNTs in purified materials.

Optical absorbance shows that our new purification method increases SWNT content relative to other carbonaceous species. For these studies, samples are annealed at 900 °C for 5 h in vacuum to heal defects that can influence the absorbance spectrum.<sup>17</sup> Samples are then sonicated in DMF for 3 h to a concentration of 0.01 mg/mL. Following the rapid SWNT-purity assessment method of Landi et al.,<sup>20</sup> we

obtain the ratio of absorbance values for the peak maxima of  $S_{22}$  and  $M_{11}$  bands,  $A_{S_{22}}:A_{M_{11}}$ , as indicated in Figure 3a and substitute them into the empirical fitting equation for arc-SWNT in the paper. We find the absolute SWNT mass fraction in the carbonaceous material increases from  $50 \pm 7\%$  in the pretreated sample to  $71 \pm 7\%$  in the magnetically purified sample. The measured increase in the nanotube content is consistent with the result from the relative evaluation method of Itkis et al.<sup>21</sup> Using the integrated peak-to-background strength at the  $S_{22}$  peak, choosing spectral cutoffs at 0.96 and 1.46 eV, we find the peak-to-background ratio increases from 0.112 in the pretreated material to 0.175 in the magnetically purified materials, which is an  $\sim 50\%$  increase in the relative nanotube content.

In Figure 3b, buckypapers of pretreated and purified material are compared by XRD. When normalized to the intensity of the graphitic onion peak ( $2\theta = 25.6^\circ$ ),<sup>4</sup> the intensity of the SWNT rope peak ( $2\theta = 5.6^\circ$ ) in the magnetically purified sample is 2.4 times greater after purification than the intensity of the same peak prior to purification. The sharp peak at  $2\theta = 26.2^\circ$  due to multiwall nanotubes (MWNTs) is present only in the pretreated spectrum, indicating efficient removal during purification.<sup>22</sup> MWNTs, which tend to grow from large catalyst particles, would be easily attracted to iron granules during magnetic filtration. These XRD results indicate increased SWNT content relative to other graphitic carbon species, in accord with the optical absorbance data.

The filling of SWNTs with  $C_{60}$  fullerenes can provide a qualitative measure of SWNT cleanliness. Prior work has shown that efficient filling of carbon nanotubes requires open tubes and a clean surface.<sup>23</sup> Here, filling is accomplished by annealing at 650 °C for 6 h under conditions previously reported.<sup>24</sup> In Figure 3c, XRD of powder samples shows a strong reduction in the intensity of the (10) SWNT rope peak

- (21) Itkis, M. E.; Perea, D. E.; Niyogi, S.; Rickard, S. M.; Hamon, M. A.; Hu, H.; Zhao, B.; Haddon, R. C. *Nano Lett.* **2003**, *3*, 309.  
 (22) Zhou, O.; Fleming, R. M.; Murphy, D. W.; Chen, C. H.; Haddon, R. C.; Ramirez, A. P.; Glarum, S. H. *Science* **1994**, *263*, 1744.  
 (23) Smith, B. W.; Luzzi, D. E. *Chem. Phys. Lett.* **2000**, *321*, 169.  
 (24) Smith, B. W.; Russo, R. M.; Chikkannanavar, S. B.; Luzzi, D. E. *J. Appl. Phys.* **2002**, *91* (11), 9333.



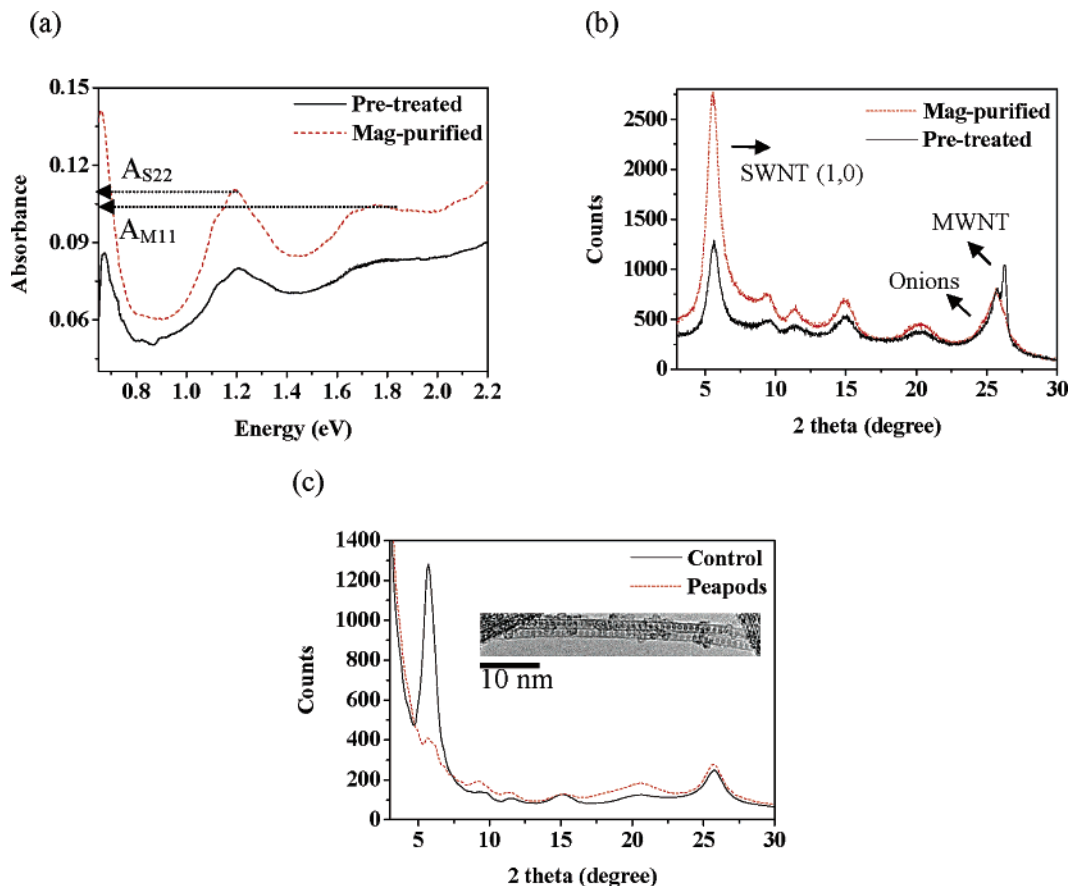


**Figure 3.** (a) NIR absorption spectra for the SWNT-content estimation. (b) XRD of the pretreated (black line) and the magnetically purified samples (red line). (c) XRD patterns of the purified SWNT control sample and the peapod sample for evaluation of the  $C_{60}$  filling efficiency. Inset shows a typical TEM micrograph of the peapods.

( $2\theta = 5.6^\circ$ ) after filling. This signal attenuation, which arises due to interference between the structure factor of the hexagonal lattice of SWNT bundles and the Bessel function of the form factor of  $C_{60}$ , can be used to calculate the fraction of filled nanotubes.<sup>25</sup> In the present case, we calculate a filling fraction of 95%. This high value indicates that the SWNTs in the material are clean, especially at open ends and large side-wall defects,<sup>23</sup> and that the interior diameter of PII-SWNTs is sufficiently large to accommodate  $C_{60}$ . A representative TEM micrograph of the peapod sample appears in the Figure 3c inset, showing dense filling of SWNTs with  $C_{60}$ .

The magnetically purified SWNT materials produced in the current work, which have as low as 50 ppm of remnant ferromagnetic Ni-enriched catalyst particles and are diamagnetic, should be suitable for a number of experiments that have historically been difficult to conduct. Figure 4 shows the high-resolution  $^{13}\text{C}$  MAS NMR data recorded on the magnetically purified powder. The isotropic chemical shift of the  $\text{sp}^2$  carbon is observed at 116 ppm referenced to TMS, which is in good agreement with previous experimental and theoretical values.<sup>5,6,18,26</sup> A reduction of the full width at half-maximum of the isotropic line from typically 50 ppm

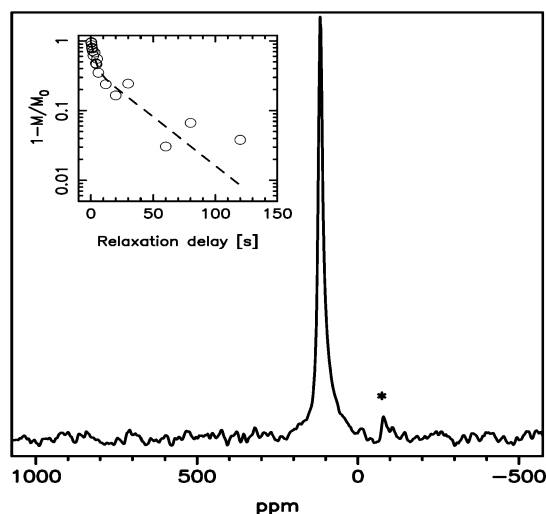


**Figure 4.** High resolution  $^{13}\text{C}$  MAS NMR spectrum of the magnetically purified sample at room temperature. The inset presents the magnetization recovery as a function of relaxation delay. The limited number of sidebands (single) shows a chemical shift anisotropy typical for  $\text{sp}^2$  carbon and no additive source of broadening, which is consistent with a high-quality material.<sup>6</sup>

according to the literature<sup>5,6,18</sup> down to 25 ppm is consistent with a low content of magnetic impurities in our materials. The inset of Figure 4 presents the magnetization recovery after saturation as a function of the relaxation delay at room temperature. Because the nuclear spin lattice relaxation time  $T_1$  of the carbon is sensitive to the presence of conduction electrons, a faster relaxation is expected for metallic nano-

(25) Kataura, H.; Maniwa, Y.; Abe, M.; Fujiwara, A.; Kodama, T.; Kikuchi, K.; Imahori, H.; Misaki, Y.; Suzuki, S.; Achiba, Y. *Appl. Phys. A* **2002**, *74*, 349.

(26) Besley, N. A.; Titman, J. J.; Wright, M. D. *J. Am. Chem. Soc.* **2005**, *127*, 17948.

tubes compared to semiconducting nanotubes.<sup>5,18</sup> Our data are consistent with a double exponential decay where  $T_1 = 2.9$  s and  $T_1 = 31$  s in metallic and semiconducting SWNTs, respectively.

### Discussion

Magnetization studies confirm that magnetic gradient filtration effectively reduces ferromagnetic impurity content in SWNT material to 0.013 emu/g. We obtain a rough estimate of ferromagnetic metal content by initially assuming that the ferromagnetic component arises from Ni with a saturation moment of  $\sim 50$  emu/g (the value for bulk Ni).<sup>27</sup> The corresponding ferromagnetic metal content is then  $\sim 50$  ppm, which is much smaller than the residual weight of the samples after carbon is removed during TGA measurements.

To understand this discrepancy, we note that TGA measures total metallic content, regardless of whether or not that material is ferromagnetic. Because PII-SWNTs are produced under conditions far from equilibrium, one may expect catalyst metallic composition will vary on the basis of local conditions during synthesis and that deviations from the phase rule probably exist.<sup>28</sup> For the pretreated sample, EDS shows that TGA residues after heating in air to 1000 °C have a Ni:Y atomic ratio of 20:1. In such samples, one expects the majority of catalyst particles to be ferromagnetic.<sup>29</sup> In contrast, TGA residues from the magnetically purified materials contain lower Ni:Y ratios of 2:1. It is known that Y rich Y–Ni alloys show very weak itinerant ferromagnetism, or Pauli paramagnetism, depending on the Y content and temperature,<sup>30</sup> Ni<sub>2</sub>Y, Ni<sub>3</sub>Y, Ni<sub>7</sub>Y<sub>2</sub>, and Ni<sub>5</sub>Y are all paramagnetic at room temperature. In the magnetically purified materials, it can be reasonably assumed that the composition of the nanoparticles varies over some range. Most of the particles with average or higher Y content would provide a paramagnetic contribution, whereas the small number of remaining Ni-rich particles would be weakly ferromagnetic consistent with the data.

With these purified samples, we can also make some estimates of SWNT diamagnetic susceptibility, which may be compared with theory. From the slope of the magnetization curves, the overall sample susceptibility is  $-2.1 \times 10^{-6}$  emu/g for pretreated samples, and  $(-2.9 \pm 0.42) \times 10^{-6}$  emu/g for magnetically purified samples at room temperature. Because it is impossible to accurately estimate the contents of MWNT and paramagnetic catalysts in the pretreated material, which is a significant factor for the determination of the diamagnetic susceptibility of SWNT, we focus on the magnetically purified materials. From optical absorbance, we

estimate SWNT content to be  $71 \pm 7$  wt % in magnetically purified materials. Carbon impurities in the magnetically purified material consist of amorphous carbon and graphitic onions as confirmed by XRD and TEM. The graphitic onion content was calculated to be  $6 \pm 1$  wt % from XRD, TGA, and TEM. The remaining content,  $22 \pm 7$  wt %, is most likely amorphous carbon. The susceptibilities of amorphous carbon and graphitic onion are approximately  $0.2 \times 10^{-6}$  and  $-2.1 \times 10^{-6}$ , respectively.<sup>31,32</sup> Pure Y has a paramagnetic susceptibility of  $187 \times 10^{-6}$  emu/g at room temperature.<sup>33</sup> Assuming 0.5 wt % pure Y in the sample, this accounts for  $\sim 1 \times 10^{-6}$  emu/g of the observed signal. Assuming that the purified material is composed of these four constituents, the resultant calculated susceptibility for SWNTs is approximately  $-5 \times 10^{-6}$  emu/g. Analytical theory shows the magnetic susceptibility of SWNTs scales with radius<sup>34</sup> and is highly sensitive to carrier concentration due to Van Hove singularities in the band structure. A zero-doping, zero-temperature, orientationally averaged estimate of SWNT diamagnetism for a mean diameter of 1.4 nm is approximately  $-0.64 \times 10^{-6}$  emu/g. This value is well below our measurement, although temperature and doping can affect this theoretical estimate significantly.

### Conclusion

Numerous spectroscopies such as ESR and NMR require highly pure SWNT samples. We describe a new purification method of single-wall carbon nanotube materials, air oxidation–hydrochloric acid treatment followed by magnetic filtration, which reduces the ferromagnetic catalyst content by nearly 2 orders of magnitude. Moreover, we find the new purification method significantly increases SWNT content relative to pretreated materials and yields clean surfaces suitable for filling experiments. Although the current yield is  $\sim 5$  mg/h because of the laboratory-scale experimental setup, there should be no limiting factor for mass-production as long as large volume SWNT dispersions are stable and a sufficient magnetic field can be generated.

**Acknowledgment.** We acknowledge financial support from NSF DMR-01-00273 and NSF-MRSEC DMR-05-20020. We are grateful for stimulating discussions and experimental assistance from Dr. J. E. Fisher, Dr. D. M. Yates of the Penn Regional Nanotech Facility (PRNTF), Dr. W. Zhou, and Dr. K. Byon. The PRNTF is partially supported by the Penn NSF-MRSEC through Grant DMR-05-20020.

CM063006H

- (27) Billas, I. M. L.; Chatelain, A.; de Heer, W. A. *Science* **1994**, *265*, 1682.  
 (28) Yudasaka, M.; Sensui, N.; Takizawa, M.; Bandow, S.; Ichihashi, T.; Iijima, S. *Chem. Phys. Lett.* **1999**, *312*, 155.  
 (29) Lienard, A.; Rebouillat, J. P. *J. Appl. Phys.* **1978**, *49* (3), 1680.  
 (30) Gignoux, D.; Lemaire, R.; Molho, P.; Tasset, F. *J. Appl. Phys.* **1981**, *52* (3), 2087.

- (31) Takai, K.; Oga, M.; Enoki, T.; Taomoto, A. *Diamond Relat. Mater.* **2004**, *13*, 1469.  
 (32) Andersson, O. E.; Prasad, B. L. V.; Sato, H.; Enoki, T.; Hishiyama, Y.; Kaburagi, Y.; Yoshikawa, M.; Bandow, S. *Phys. Rev. B* **1998**, *58* (24), 16387.  
 (33) Gardner, W. E.; Penfold, J.; Taylor, M. A. *Proc. Phys. Soc.* **1965**, *85*, 963.  
 (34) Lu, J. P. *Phys. Rev. Lett.* **1995**, *74* (7), 1123.